coatings

MDPI

Article

Synthesis and Composition Study of Electrochemically Deposited Ni-P Coating with Increased Surface Area

Sergey S. Perevoznikov [1], Ilya V. Yakovlev [2,*], Ludmila S. Tsybulskaya [1] and Olga B. Lapina [2,*]

[1] Research Institute for Physical Chemical Problems, Belarusian State University, 14, Leningradskaya Street, 220030 Minsk, Belarus; perevoznikovs@yandex.by (S.S.P.); tsybul@bsu.by (L.S.T.)
[2] Boreskov Institute of Catalysis, 5, Prospekt Lavrentieva, 630090 Novosibirsk, Russia
* Correspondence: iv_yakovlev@catalysis.ru (I.V.Y.); olga@catalysis.ru (O.B.L.); Tel.: +73-8332-69-505 (I.V.Y.)

Abstract: Nickel phosphides Ni_xP_y are a promising family of binary compounds that have shown much promise in various fields of technology, including energy storage, light absorption and heterogeneous catalysis in the reactions of biomass hydrogenation. The performance of Ni_xP_y-containing materials depends greatly on their morphology and phase composition and, in turn, on the synthesis technique. In this work, we have employed the electroplating approach to synthesize a Ni-P coating, which was treated with nitric acid in order to develop its surface area and enrich it with phosphorus. We have employed scanning electron microscopy, X-ray diffraction and ^{31}P nuclear magnetic resonance techniques to characterize the particles separated from the coating with ultrasound for the convenience of the study. According to experimental data, the obtained powder contained a mixture of Ni_3P and phosphorus oxides, which transformed into nickel phosphide phases richer with phosphorus, such as Ni_5P_2 and $Ni_{12}P_5$, after treatment at elevated temperatures. Thus, we have demonstrated that electroplating followed by acid treatment is a feasible approach for the synthesis of Ni-P coatings with increased surface area and variable phase composition.

Keywords: nickel phosphide coating; electroplating; ^{31}P Solid-State NMR

Citation: Perevoznikov, S.S.; Yakovlev, I.V.; Tsybulskaya, L.S.; Lapina, O.B. Synthesis and Composition Study of Electrochemically Deposited Ni-P Coating with Increased Surface Area. *Coatings* **2021**, *11*, 1071. https://doi.org/10.3390/coatings11091071

Academic Editor: Giovanni Zangari

Received: 6 August 2021
Accepted: 3 September 2021
Published: 5 September 2021

1. Introduction

Nickel phosphides are a family of binary compounds of nickel and phosphorus, the atomic ratio of which can vary over a wide range from 3:1 to 1:3 [1]. All nickel phosphides have a metallic conductivity character; most of them are characterized by Pauli paramagnetism. The nickel-rich side of this spectrum (Ni:P > 1) has attracted more research interest because the nickel-rich phases have found practical applications in various fields of technology. Nickel phosphides and composite materials based on them are used as anode materials for lithium-ion batteries [2–5], light-absorbing surfaces of optical devices [6,7]. Much attention is currently focused on studying the possibility of using nickel phosphides in the field of heterogeneous catalysis in biomass hydrotreating reactions. Namely, nickel phosphides Ni_3P, $Ni_{12}P_5$, Ni_2P and Ni_5P_4 are promising catalysts for hydrodeoxygenation [8–10], hydrodesulfurization [11–16] and other hydrogenation processes [17–20], due to their higher activity and stability compared to catalysts based on purely metallic Ni.

The properties of nickel phosphides in these fields of interest are greatly influenced by their morphology and phase composition. Therefore, in the literature, attention is paid not only to the study of the properties of various phases of nickel phosphides but also to the development of methods for their synthesis [2,11,12,16,21,22]. The most common among them are the methods of incipient wetness impregnation with compounds of nickel and phosphorus, followed by their reduction in a temperature-programmed mode in a vacuum or a reducing environment; direct phosphine treatment of supported Ni or NiO nanoparticles is also used [23].

Earlier, we have shown that electrochemically deposited Ni-P coatings can contain from 1.5 to 21.5 at.% phosphorus and represent either an interstitial-substitutional type solid

solution of phosphorus in nickel (1.5–9.0 at.% P) or an X-ray amorphous phase (coatings with more than 9 at.% phosphorus) [24]. After heating of the as-deposited Ni-P coating in the temperature range of 350–400 °C, a thermally stimulated phase transformation occurs with the formation of metallic nickel and nickel phosphide Ni_3P phases, the volume fraction of the latter being determined by the phosphorus content in the coating [25]. Since the maximum phosphorus content in the Ni-P coating does not exceed 21.5 at.%, and the phase composition after heating is determined by the chemical composition [25], nickel phosphide phases richer in phosphorus were not obtained. At the same time, obtaining a Ni-P coating with a wider composition range that would include Ni_xP_y phases with a lower x/y ratio may prove beneficial because, depending on the application area, such phases can demonstrate higher efficiency. For example, Ni_2P and $Ni_{12}P_5$ demonstrate higher activity in catalytic hydrodeoxygenation of fatty acid esters [9]. It was shown in [26,27] that an increase in the phosphorus content on the coating surface can be achieved by treating it in a nitric acid solution. However, the phase composition and structure of the surface layers enriched in phosphorus are poorly studied [28], and the possibility of obtaining nickel phosphide phases as a result of heating the treated coatings has not been investigated either.

In this work, we have electrochemically deposited a Ni-P coating on a copper foil and treated it with nitric acid in order to enrich its surface with phosphorus. We have employed scanning electron microscopy to study the morphology of the obtained surface, which consisted of micron-sized ternary Ni-P-O conical particles supported on the Ni-P substrate. An X-ray diffraction technique combined with solid-state ^{31}P nuclear magnetic resonance spectroscopy allowed us to establish the nickel phosphide and nickel phosphate phases present in the obtained particles and to report the Knight shifts of phosphorus sites of nickel phosphide Ni_5P_2. Heating of the particles separated from the substrate to 800 °C in vacuum led to crystallization of nickel phosphide nanoparticles surrounded by a nickel phosphate shell.

2. Materials and Methods

The Ni-P coating was deposited on a 50 × 25 mm^2 copper foil from an electrolyte with the following composition: $NiSO_4 \cdot 7H_2O$ (180 g/L), $NiCl_2 \cdot 6H_2O$ (10 g/L), H_3PO_4 (10 g/L), KH_2PO_4 (14 g/L), H_3PO_3 (20 g/L), saccharin (2 g/L), pH 2. The deposition was carried out in an electrochemical cell under constant temperature (60 ± 1 °C) with vertical oscillation of the cathode with a frequency of 30 min^{-1}. Cathode current density of 3 A/dm^2 was applied for 2 h until a smooth coating (Figure 1) with the thickness of 45–50 μm was reached. During the deposition, the pH of the electrolyte was maintained at the same level (pH 2) by adding concentrated H_2SO_4. The thickness of the coating was determined by the gravimetric method. The phosphorus content in the coating was estimated by the X-ray fluorescence method using an Epsilon 1 spectrometer (PANalytical, Almelo, the Netherlands). Automatic data processing was performed using Epsilon 3 software using the Stratos application.

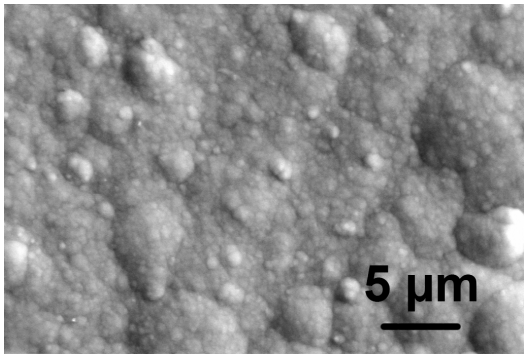

Figure 1. SEM micrograph of the as-deposited Ni-P coating. Note the relatively smooth surface of the coating prior to the acidic treatment.

The surface oxidation of Ni-P coatings was carried out by keeping the samples in a 5 M solution of nitric acid for 150–170 s at 55 °C. The study of the morphology of the coating surface was carried out using a Tescan Vega 3 scanning electron microscope (TESCAN ORSAY HOLDING, Brno, Czech Republic) equipped with a secondary electron detector (for studying the surface morphology) and a reflected electron detector (for phase contrast detection). A Leo 1455 scanning electron microscope (Carl Zeiss AG, Oberkochen, Germany) with an X-ray fluorescent attachment was used to determine the chemical composition of the surface. X-ray diffraction experiments (XRD) were carried out using an Empyrean X-ray diffractometer (PANalytical, Almelo, the Netherlands) with CuK_α radiation (Ni-filter) equipped with an attachment allowing X-ray diffraction patterns to be recorded at elevated temperatures in a vacuum (10^{-4} Torr). The duration of heating at each selected temperature was 30 min.

Thermal analysis (thermogravimetric analysis with scanning differential calorimetry (DSC)) was performed using an STA449-F3 Jupiter simultaneous thermal analyzer (Netzsch, Selb, Germany) at a sample heating rate of 10 K/min in a nitrogen atmosphere using a Pt/Rh crucible in a temperature range from 30 to 850 °C.

The specific surface area of the as-separated powder was characterized using N_2 physisorption at 77 K with an ASAP 2400 system (Micromeritics, Norcross, GA, USA). The specific surface area was determined using a multipoint Brunauer–Emmett–Teller (BET) model.

13 kHz magic angle spinning (MAS) ^{31}P nuclear magnetic resonance (NMR) spectra were recorded using a Bruker AVANCE III Fourier spectrometer (Bruker, Billerica, MA, USA) with a constant magnetic field of 11.74 T. The spectra were recorded at the 202.404 MHz Larmor frequency of the ^{31}P nuclei using a $\pi/2$-τ-π Hahn echo sequence. The samples were placed in a 4 mm (outer diameter) ZrO_2 rotor. Twenty-seven and thirty kHz MAS ^{31}P NMR spectra were recorded on a Bruker AVANCE 400 Fourier spectrometer in a constant magnetic field of 9.4 T (162.1 ^{31}P Larmor frequency). For these experiments, the sample was placed in a 2.5 mm outer diameter ZrO_2 rotor. All sample manipulations were carried out under open atmosphere.

In all cases, the $\pi/2$ pulse length was 2.4 μs and the interpulse delay was chosen such that the experiments were rotor-synchronized. Due to the rapid relaxation of P sites in intermetallic compounds, a short delay (0.05 s) between the pulse sequences was chosen. Echo-mapping procedure with a ~100 kHz carrier frequency step was used to record the spectra severely broadened (spanning over 7000 ppm) due to the presence of paramagnetic ions. To record ultra-wide lines caused by the conducting or paramagnetic character of the systems under study, the echo-mapping procedure was used. In this case, the detuning of the carrier frequency was changed with a step of 500 ppm, which corresponds to ~100 kHz at a given Larmor frequency. All NMR spectra were recorded at room temperature and referenced to an 85% H_3PO_4 solution.

3. Results and Discussion

The Ni-P coating with a phosphorus content of ~5.0 at.% was synthesized by electrochemical deposition. Treatment of this coating in a nitric acid solution led to its partial dissolution with the formation of a deep black surface. Analysis of the composition of this surface, carried out using an EDX attachment of a scanning electron microscope, showed the presence of elements in the following concentrations, at.%: nickel-56.7, oxygen-30.7, phosphorus-11.8, sulfur-0.8. The coating contained a small amount of sulfur due to the saccharin present in the electrolyte. The drastic change in the Ni:P ratio from 1:20 to 1:4.8 indicates the predominant removal of nickel from the surface during the etching of the Ni-P coating in nitric acid and the accumulation of phosphorus. At the same time, the presence of a large amount of oxygen in the surface layer indicates the presence of oxidized species at the surface.

In [7,29], it was shown that the treatment of chemically or electrochemically deposited Ni-P coatings in a nitric acid solution leads to the formation of a well-developed micro-

relief of the surface, which significantly increases its specific area. From the micrographs obtained with the use of a secondary electron detector, we could observe that the etching of Ni-P coatings had resulted in a surface with regularly alternating cone-shaped elements (Figure 2a,b). The diameter of the base of the cones was 2–3 μm and their height was 6–8 μm. The tops of the cones appeared with slightly higher brightness, which indicates poor drainage of the charge accumulated in these areas during irradiation with electrons and, accordingly, their dielectric nature.

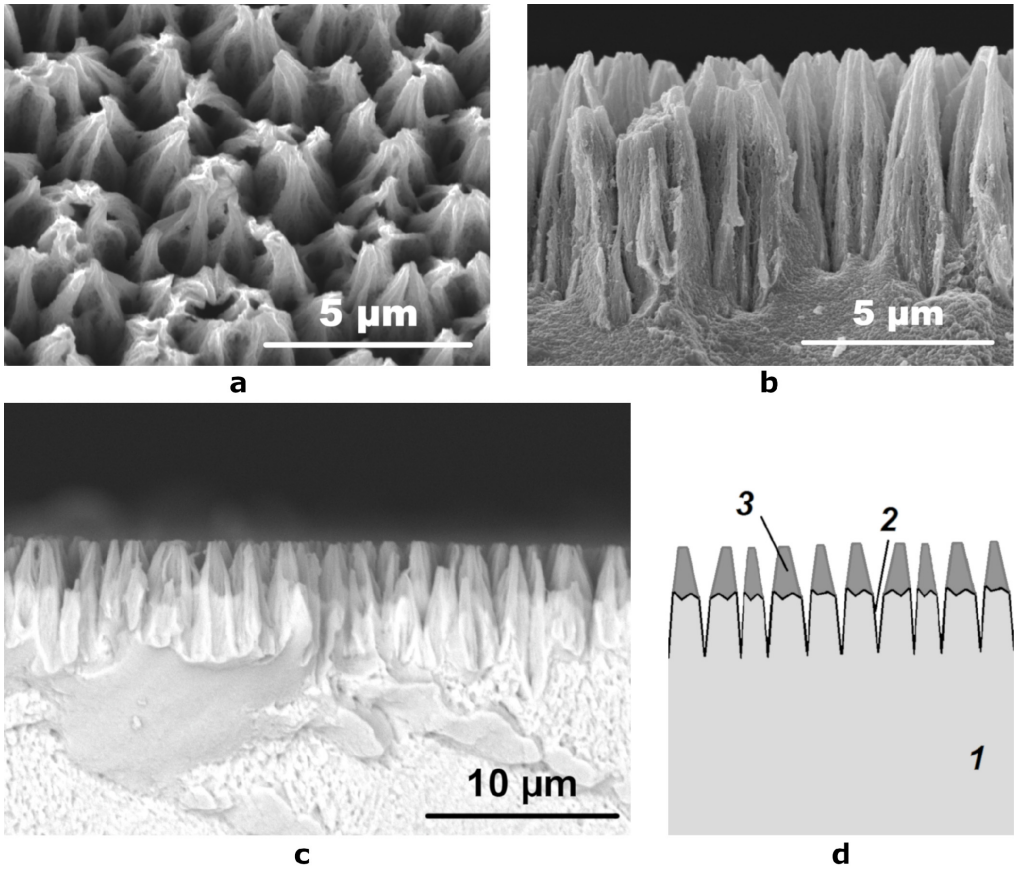

Figure 2. SEM micrographs of (**a**) the etched surface at an angle of 10° and (**b**) its cross section obtained using a secondary electron detector; (**c**) a cross section SEM image obtained using a reflected electron detector; (**d**) schematic representation of the cross section of the etched coating: 1—Ni-P coating, 2—hollows formed during etching, 3—layer of conical particles containing light elements.

When studying the cross section of the etched coating using a backscattered electron detector, we have found that the distribution of elements in it is non-uniform (Figure 2c). Between the tops of the cones (2–3 microns) and their lower part (4–5 microns), there is a clear border in the brightness of the image. The upper part has a low signal intensity, which indicates the presence of a large amount of light elements in its composition, while the lower part has the same signal intensity as the Ni-P coating on the substrate, which was not etched, which indicates that their composition is very close. The schematic structure of the oxidized surface is shown in Figure 2d.

Due to the small thickness of the topmost layer on the etched surface (Figure 2c), it was separated from the substrate in the form of a fine powder in order to determine its chemical composition. For this, the etched Ni-P coatings were placed in a container with a minimum amount of ethanol and subjected to ultrasonic treatment to obtain a suspension of black powder in alcohol. After the evaporation of the alcohol at 40 °C, the fine powder was dried in air and stored in a desiccator. According to the scanning electron microscopy data, the powder consisted of conical particles 2.5–4.0 μm in length

and 1.0–2.0 μm in diameter at the base (Figure 3a). Consequently, the ultrasonic treatment with separation of conical particles led to smoothing of the surface of the etched Ni-P coating: SEM micrographs of the treated surface revealed that the upper pointed parts of the cone-shaped elements disappeared, while numerous hollows significantly differing in size are observed (Figure 3b). The obtained black powder displayed a moderate specific surface area of 53 m^2/g according to a BET adsorption study. Due to the smoothness of the as-obtained coating (Figure 1), we can follow geometrical considerations to evaluate the specific surface area increase provided by the nitric acid treatment. From 1 dm^2 of Ni-P coating, we can separate roughly 20 mg of powder that, considering the BET measurement results, has a total surface of 1.06 m^2 resulting in a 100-fold increase of surface area.

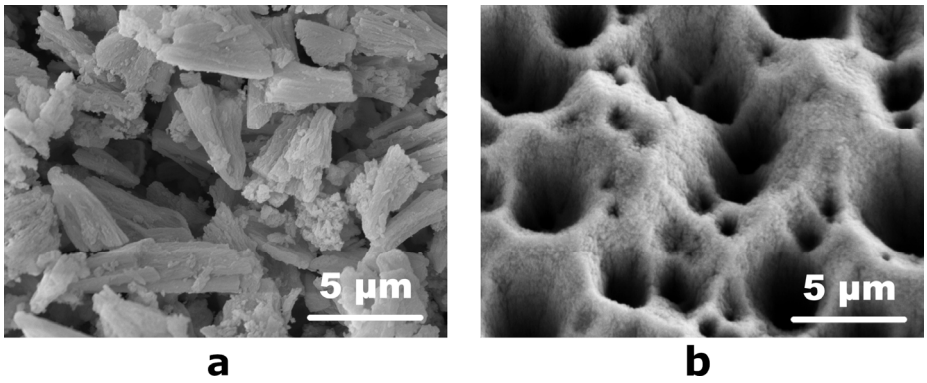

Figure 3. SEM micrographs of (**a**) the separated fine powder (note the conical shape of the particles that has not changed during the ultrasonic treatment) and (**b**) the etched surface after the ultrasonic treatment.

To investigate the phase composition of the obtained powder, a study was carried out using the X-ray diffraction technique. The XRD pattern shown in Figure 4a shows two broad halo peaks characteristic of amorphous materials. The first of them is located in the range of angles $2\theta = 27°–37°$ and the second is located in 41°–47° region. Such a large width of reflections can be due to both the amorphous state of the substance and the very small size of the coherent scattering regions. Thus, the XRD technique turned out to be uninformative in identification of compounds present in the upper layer of the separated powder.

Unlike the XRD technique, the NMR technique is much less sensitive to the particle (and crystallite) size and allows one to study the structure of amorphous materials. The 13 kHz magic angle spinning ^{31}P NMR spectrum of the obtained powder (Figure 4b) shows a broad line shape with two distinguishable regions: the region of signals from diamagnetic phosphorus compounds (in vicinity of 0 ppm) and the region of signals shifted to a weak field (about 1500 ppm). Such a large signal shift (Knight shift) has several possible sources: for non-conducting compounds it is caused by the presence of spin density from electrons of paramagnetic centers Ni (most often, Fermi contact shift); for conducting compounds, by the presence of conduction electrons; for conducting materials with paramagnetic ions, a combination of both sources may be present. The signals are highly broadened and cannot be resolved. However, due to the presence of signals in the diamagnetic region, it can be argued that a noticeable proportion of phosphorus is present in the oxide form. These signals can correspond to various phosphate groups (PO_4, P_2O_7, PO_3, etc.), in the immediate environment of which there are no paramagnetic nickel ions. Such groups can be part of various di-, tri- and polyphosphoric acids, which can be products of phosphorus oxidation in a strongly acidic medium. This is in good agreement with the elemental analysis data on the presence of a large amount of oxygen in the Ni-P coating after its etching in nitric acid. Moreover, the broad character of the spectrum does not allow for excluding the presence of elemental phosphorus in the sample. Signals in the region of large Knight shifts seem to correspond to nickel-rich phosphide phases, namely, Ni_3P or

$Ni_{12}P_5$, the signals which are located at about 1800 ppm for the Ni_3P phase and about 1950 and 2250 ppm for the $Ni_{12}P_5$ phase [30,31].

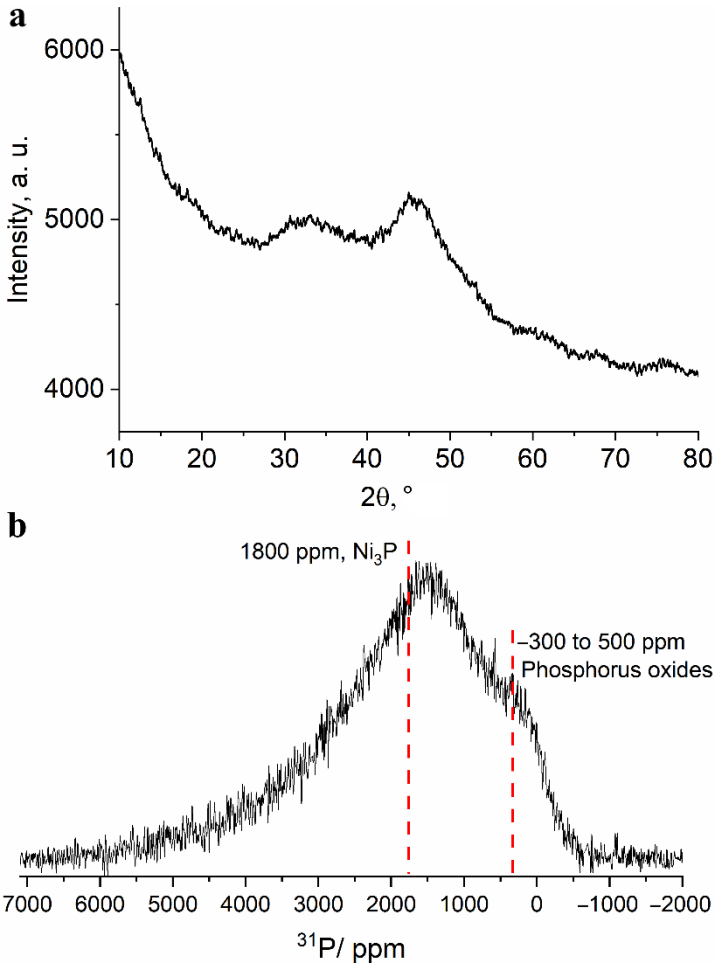

Figure 4. (**a**) Fragment of an X-ray diffraction pattern and (**b**) 13 kHz MAS ^{31}P NMR spectrum obtained for the separated fine powder.

The significant broadening of the spectrum and its "distributed" nature may indicate the presence of nonstoichiometric defect phases of phosphides and nickel phosphates. In order to confirm the presence or absence of the latter, we have synthesized and recorded ^{31}P MAS NMR spectra of several pure nickel phosphates (article in preparation) because only nickel pyrophosphate $Ni_2P_2O_7$ was covered in the literature with the reported Knight shift of 3950 ppm [32]. Despite their insulating character, the signals of synthesized phosphates cover ^{31}P Knight shifts in a wide range from 1000 to 8000 ppm. Nickel orthophosphate $Ni_3(PO_4)$ gives rise to a broad line stretching from 1000 to 3000 ppm, which fits well within the experimental spectrum of the fine powder. The low-field "tail" of the spectrum extending into the 4000–5000 ppm region may indicate the presence of highly disordered δ-$Ni_2P_2O_7$ phase that gives rise to a signal centered around 3900 ppm. Thereby, according to ^{31}P NMR data, the separated fine powder comprises Ni-rich phosphide and phosphate phases with some of the phosphorus present as phosphoric and polyphosphoric acids or in an elemental state.

Crystallization and ordering of the formed phases can be achieved by heating the powder in an inert atmosphere to prevent oxidation of nickel and phosphorus. To determine the temperatures at which structural-phase transformations of a fine powder occur, a study was carried out using the differential scanning calorimetry technique. From the thermal analysis curve shown in Figure 5, it follows that when the powder is heated in a

nitrogen atmosphere from 25 to 500 °C, its weight decreases by 21.7%, the process proceeds with heat absorption and has a peak on the DSC curve at 126 °C. The rapid weight loss observed up to 200 °C may be due to the removal of the adsorbed water from the powder. Further delayed weight reduction may be associated with the polyphosphoric acid polycondensation processes occurring during heating. Two exothermic peaks are observed on the DSC curve: one of low intensity with a maximum at 400 °C, and the other, a narrow, sharp one at 755 °C. We assume from the XRD data presented below that the former peak corresponds to the crystallization of nickel phosphides, while the latter peak corresponds to the crystallization of nickel phosphates. No change in the mass of the sample in the temperature range from 500 to 730 °C was recorded (Figure 5).

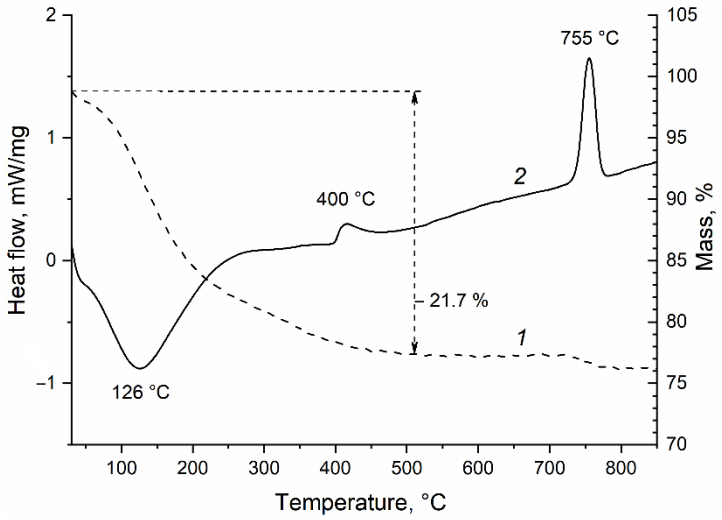

Figure 5. Thermogravimetry (1) and differential scanning calorimetry (2) curves of the separated fine powder when heated in nitrogen.

To study the structural transformations during heating of the obtained powder, the following temperatures were chosen: 500 and 800 °C. The X-ray diffraction patterns of the powder heated to 500 °C show several intense reflections corresponding to nickel phosphide phases $Ni_{12}P_5$ and Ni_5P_2 (Figure 6a). The large broadening of the reflections indicates either the small size of the crystallites or their high defectiveness. In the 13 kHz ^{31}P NMR spectrum of the powder heated at 500 °C, one can observe a significant decrease in the signals in the diamagnetic region of the spectrum, simultaneous with the growth of the broad spectrum shoulder in the region of 3000–5000 ppm (Figure 6b). Thus, it can be assumed that, upon heating, amorphous polyphosphates interact with nickel to form nickel phosphides or nickel phosphates. A line that cannot be attributed to any previously studied nickel phosphate or phosphide is relatively well defined at approximately 1200 ppm. Considering the data obtained by XRD, this line may correspond to the Ni_5P_2 phase. Even at this temperature, the lines in the spectrum are notably broad, which indicates a significant disorder or defectiveness of these compounds (Figure 6b).

After heating the powder at 800 °C, the entire set of narrow reflections from nickel phosphides $Ni_{12}P_5$ and Ni_5P_2 became clearly visible in the X-ray diffraction patterns, which indicates their good crystallization. Intense narrow reflections from metaphosphate $Ni(PO_3)_2$ and nickel pyrophosphate $Ni_2P_2O_7$ also appeared (Figure 7a). The detection of these phosphates may be due to their crystallization from the amorphous state, which may be the exothermal process reflected in the peak at 755 °C on the DSC curve. The ^{31}P NMR spectrum demonstrates a noticeable narrowing of the lines, for which the specific Knight shifts can be attributed. The intensity of the signals in the 0 ppm region decreased drastically, which indicates the complete conversion of "free" phosphates into compounds with nickel. Lines with shifts of about 1200, 2250, 4000 and 5000 ppm can be distinguished in the spectrum (Figure 7b). The line at 4000 ppm can be attributed to nickel pyrophosphate

(δ-phase), the presence of which was also confirmed by XRD data. Nickel phosphide phase Ni_2P gives rise to a line located in the same region; however, the absence of this phase in the sample is evident from the absence of a line at 1500 ppm from the second phosphorus site in the Ni_2P structure [30,31,33]. The line located at 2250 ppm confirms the presence of the nickel phosphide phase $Ni_{12}P_5$ detected by XRD. According to our measurements made for reference nickel phosphates, the signal at 5000–6000 ppm corresponds to α-modification of $Ni_2P_2O_7$.

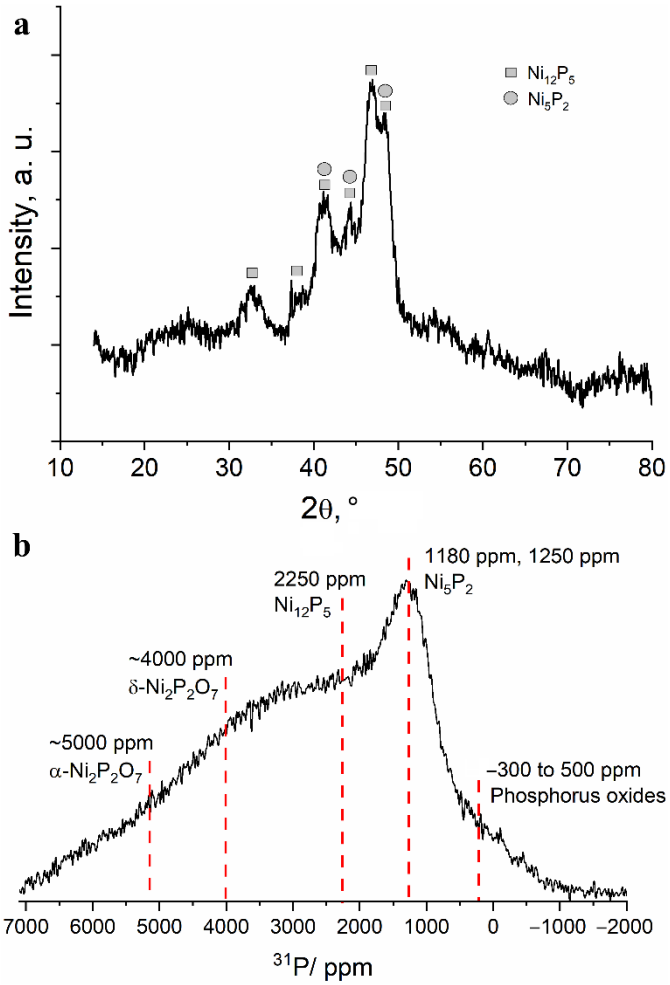

Figure 6. (**a**) Fragment of an X-ray diffraction pattern and (**b**) 13 kHz MAS ^{31}P NMR spectrum obtained for the separated fine powder after heating at 500 °C in vacuum.

Nickel metaphosphate $Ni(PO_3)_2$ gives rise to a weakly intensive line at 7000 ppm, severely broadened due to the strong paramagnetic influence of Ni ions that can also lead to quick relaxation of ^{31}P nuclear magnetization to its equilibrium state. Thus, although weak $Ni(PO_3)_2$ reflexes are observed in the XRD pattern of the sample heated to 800 °C, the NMR signature of this phase is missing in the spectrum. The last line on the 13 kHz ^{31}P NMR spectrum located at approximately 1200 ppm differs significantly from the rest of the lines by clearly observable spinning sidebands. Their presence means that this line corresponds to a well-ordered phase. Taking into account the results obtained using XRD, the most probable candidate for such a phase is Ni_5P_2. In order to specify the Knight shift of this compound, we have recorded partial MAS spectra at higher rotation frequencies of 27 and 30 kHz (Figure 7c). Despite the low signal-to-noise ratio, we observed several lines that remained static between these spectra. The first two lines located at 2250 and 1950 ppm correspond to a $Ni_{12}P_5$ phase, while the two other lines at 1250 and 1180 ppm that have not been reported previously likely correspond to a Ni_5P_2 phase.

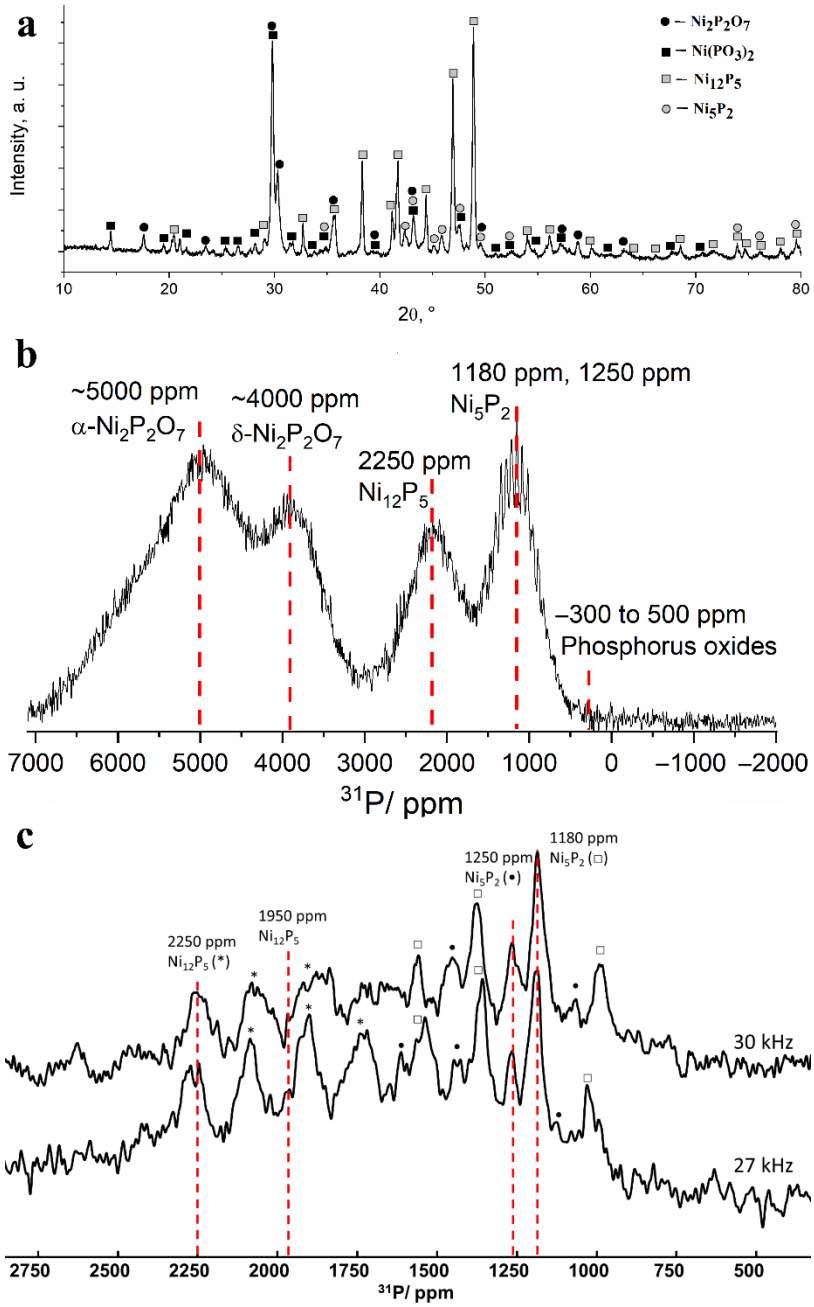

Figure 7. (**a**) X-ray diffraction pattern and (**b**) 13 kHz MAS ^{31}P NMR spectrum obtained for the separated fine powder after heating at 800 °C in vacuum. (**c**) Comparison of 30 kHz (top) and 27 kHz (bottom) MAS ^{31}P NMR spectra. Asterisk, circle and square denote the corresponding spinning sidebands of $Ni_{12}P_5$ (2250 ppm line), Ni_5P_2 (1250 ppm line) and Ni_5P_2 (1180 ppm line), respectively.

The electron microscopic investigation of the finely dispersed powder after heating in a vacuum at 800 °C demonstrated the sintering of cone-shaped particles produced by the etching of the Ni-P coating (Figure 8). In the phase contrast mode, it can be clearly seen that rounded grains of dense nickel phosphides (approximately 100 nm in diameter) that have a lighter shade in the image are evenly distributed in the mass of nickel phosphates, which have lower density (Figure 8). There are also areas in which the aggregation of nickel phosphide particles has occurred, as a result of which large light areas with a size of 300–800 nm are formed, next to which there are dark areas of nickel phosphate particles of the same size. Furthermore, the micrograph contains fragments of cone-shaped particles

that have not sintered. In these fragments, one can observe a uniform distribution of light nickel phosphide granules in the gray matrix of phosphates (Figure 8).

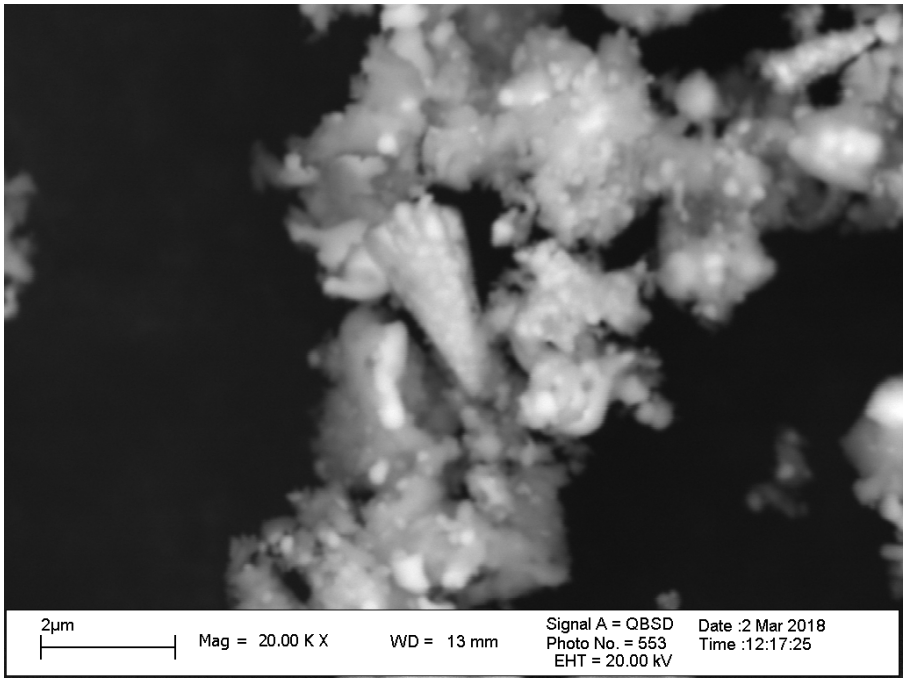

Figure 8. SEM micrograph of the separated powder heated at 800 °C in vacuum, obtained using a reflected electron detector.

4. Conclusions

A new method for the synthesis of nickel phosphide-phosphate compounds immobilized on an electrochemically deposited Ni-P coating by etching it in a nitric acid solution is proposed. The resulting surface has a developed micro-relief and consists of uniformly alternating cone-shaped elements, with a diameter of 1–2 μm at the base and a length of 4–5 μm. Nitric acid etching has successfully served as a mean to enrich the deposited surface with phosphorus. According to the elemental analysis data, the conical formations were enriched with light elements relative to the original coating with a P:Ni ratio increased from 1:20 to just about 1:5. An XRD study of the as-synthesized powder separated from the surface by ultrasonic treatment revealed no crystalline phases. At the same time, according to ^{31}P NMR data, the sample contained highly disordered nickel phosphide phases as well as phosphorus in the form of amorphous polyphosphates not bound to nickel.

After heating the cone-shaped particles in a vacuum at 500 °C, two nickel phosphide phases $Ni_{12}P_5$ and N_5P_2 are precipitated according to XRD data and precipitation of nickel phosphide phases is observed: $Ni_{12}P_5$ and Ni_5P_2. Further heating to 800 °C leads to crystallization of nickel phosphates, namely, metaphosphate $Ni(PO_3)_2$ and pyrophosphate $Ni_2P_2O_7$ (α- and δ-phases). The presence of the detected phases was confirmed by the ^{31}P NMR technique, with Knight shifts of nickel phosphide phase N_5P_2 reported for the first time. After heating at 800 °C, according to the SEM micrographs, rounded grains of nickel phosphides are evenly distributed in the matrix of nickel meta- and pyrophosphates. These results demonstrate that, even at low initial phosphorus concentrations, electrochemical deposition allows obtaining of a coating with a developed micro-relief containing nanoparticles of nickel phosphides that perform well in various technology fields, including catalyzed biomass refinement, where phases with higher P:Ni atomic ratio ($Ni_{12}P_5$ and Ni_2P) display increased catalytic performance.

Author Contributions: Conceptualization, L.S.T. and O.B.L.; methodology, L.S.T. and O.B.L.; investigation, S.S.P. and I.V.Y.; resources, L.S.T.; writing—original draft preparation, L.S.T.; writing—review and editing, S.S.P., O.B.L. and I.V.Y.; supervision, O.B.L.; funding acquisition, S.S.P. and I.V.Y. All authors have read and agreed to the published version of the manuscript.

Funding: The reported study was funded by RFBR and BRFBR according to the research project No. 19-53-04017. I.V.Y. and O.B.L. acknowledge that this work was partially supported by the Ministry of Science and Higher Education of the Russian Federation within the governmental order for Boreskov Institute of Catalysis (project AAAA-A21-121011390054-1).

Institutional Review Board Statement: Not applicable.

Informed Consent Statement: Not applicable.

Data Availability Statement: Not applicable.

Conflicts of Interest: The authors declare no conflict of interest.

References

1. Schmetterer, C.; Vizdal, J.; Ipser, H. A new investigation of the system Ni–P. *Intermetallics* **2009**, *17*, 826–834. [CrossRef]
2. Li, Q.; Ma, J.; Wang, H.; Yang, X.; Yuan, R.; Chai, Y. Interconnected Ni_2P nanorods grown on nickel foam for binder free lithium ion batteries. *Electrochim. Acta* **2016**, *213*, 201–206. [CrossRef]
3. Fullenwarth, J.; Darwiche, A.; Soares, A.; Donnadieu, B.; Monconduit, L. NiP_3: A promising negative electrode for Li- and Na-ion batteries. *J. Mater. Chem. A* **2013**, *2*, 2050–2059. [CrossRef]
4. Li, G.; Yang, H.; Li, F.; Du, J.; Shi, W.; Cheng, P. Facile formation of a nanostructured NiP2@C material for advanced lithium-ion battery anode using adsorption property of metal–organic framework. *J. Mater. Chem. A* **2016**, *4*, 9593–9599. [CrossRef]
5. Lu, Y.; Wang, X.; Mai, Y.; Xiang, J.; Zhang, H.; Li, L.; Gu, C.; Tu, J.; Mao, S.X. Ni_2P/Graphene sheets as anode materials with enhanced electrochemical properties versus lithium. *J. Phys. Chem. C* **2012**, *116*, 22217–22225. [CrossRef]
6. Brown, R.J.C.; Brewer, P.J.; Milton, M.J.T. The physical and chemical properties of electroless nickel-phosphorus alloys and low reflectance nickel-phosphorus black surfaces. *J. Mater. Chem.* **2002**, *12*, 2749–2754. [CrossRef]
7. Perevoznikov, S.S. Polucheniye ul'trachernykh plenok na osnove elektroosazhdennykh pokrytiy nikel'-fosfor. *Vopr. Him. Him. Teh.* **2011**, *4*, 116–119.
8. Shamanaev, I.V.; Deliy, I.V.; Aleksandrov, P.V.; Gerasimov, E.Y.; Pakharukova, V.P.; Kodenev, E.G.; Ayupov, A.B.; Andreev, A.S.; Lapina, O.B.; Bukhtiyarova, G. Effect of precursor on the catalytic properties of Ni_2P/SiO_2 in methyl palmitate hydrodeoxygenation. *RSC Adv.* **2016**, *6*, 30372–30383. [CrossRef]
9. Deliy, I.V.; Shamanaev, I.V.; Gerasimov, E.Y.; Pakharukova, V.P.; Yakovlev, I.V.; Lapina, O.B.; Aleksandrov, P.V.; Bukhtiyarova, G.A. HDO of methyl palmitate over silica-supported Ni phosphides: Insight into Ni/P effect. *Catalyst* **2017**, *7*, 298. [CrossRef]
10. Yu, Z.; Wang, A.; Liu, S.; Yao, Y.; Sun, Z.; Li, X.; Liu, Y.; Wang, Y.; Camaioni, D.M.; Lercher, J. Hydrodeoxygenation of phenolic compounds to cycloalkanes over supported nickel phosphides. *Catal. Today* **2019**, *319*, 48–56. [CrossRef]
11. Cho, K.-S.; Seo, H.-R.; Lee, Y.-K. A new synthesis of highly active Ni_2P/Al_2O_3 catalyst by liquid phase phosphidation for deep hydrodesulfurization. *Catal. Commun.* **2011**, *12*, 470–474. [CrossRef]
12. Song, L.; Zhang, S.; Wei, Q. A new route for synthesizing nickel phosphide catalysts with high hydrodesulfurization activity based on sodium dihydrogenphosphite. *Catal. Commun.* **2011**, *12*, 1157–1160. [CrossRef]
13. Yang, L.; Li, X.; Wang, A.; Prins, R.; Wang, Y.; Chen, Y.; Duan, X. Hydrodesulfurization of 4,6-dimethyldibenzothiophene and its hydrogenated intermediates over bulk Ni2P. *J. Catal.* **2014**, *317*, 144–152. [CrossRef]
14. Li, M.; Yehl, J.; Hou, G.; Chatterjee, P.B.; Goldbourt, A.; Crans, D.C.; Polenova, T. NMR crystallography for structural characterization of oxovanadium (V) complexes: Deriving coordination geometry and detecting weakly coordinated ligands at atomic resolution in the solid state. *Inorg. Chem.* **2015**, *54*, 1363–1374. [CrossRef] [PubMed]
15. Liu, D.; Wang, A.; Liu, C.; Prins, R. Bulk and Al_2O_3-supported Ni_2P HDS catalysts prepared by separating the nickel and hypophosphite sources. *Catal. Commun.* **2016**, *77*, 13–17. [CrossRef]
16. Liu, D.; Wang, A.; Liu, C.; Prins, R. Ni_2P/Al_2O_3 hydrodesulfurization catalysts prepared by separating the nickel compound and hypophosphite. *Catal. Today* **2017**, *292*, 133–142. [CrossRef]
17. Albani, D.; Karajovic, K.; Tata, B.; Li, Q.; Mitchell, S.; López, N.; Pérez-Ramírez, J. Ensemble design in nickel phosphide catalysts for alkyne semi-hydrogenation. *Chem. Cat. Chem.* **2019**, *11*, 457–464. [CrossRef]
18. Chen, H.; Tan, J.; Zhu, Y.; Li, Y. An effective and stable Ni_2P/TiO_2 catalyst for the hydrogenation of dimethyl oxalate to methyl glycolate. *Catal. Commun.* **2016**, *73*, 46–49. [CrossRef]
19. Wei, J.; Ni, Y.; Xiang, N.; Zhang, Y.; Ma, X. Urchin-like Ni*x*P*y* hollow superstructures: Mild solvothermal synthesis and enhanced catalytic performance for the reduction of 4-nitrophenol. *Cryst. Eng. Comm.* **2014**, *16*, 2113–2118. [CrossRef]
20. Carenco, S.; Leyva-Pérez, A.; Concepción, P.; Boissière, C.; Mézailles, N.; Sanchez, C.; Corma, A. Nickel phosphide nanocatalysts for the chemoselective hydrogenation of alkynes. *Nano Today* **2012**, *7*, 21–28. [CrossRef]

21. Song, H.; Ren, Q.; Li, F.; Song, H. Preparation of a highly dispersed Ni_2P/Al_2O_3 catalyst using Ni-Al-CO_3^{2-} layered double hydroxide as a nickel precursor. *Catal. Commun.* **2016**, *73*, 50–53. [CrossRef]
22. Guan, Q.; Cheng, X.; Li, R.; Li, W. A feasible approach to the synthesis of nickel phosphide for hydrodesulfurization. *J. Catal.* **2013**, *299*, 1–9. [CrossRef]
23. Yang, S.; Liang, C.; Prins, R. A novel approach to synthesizing highly active Ni_2P/SiO_2 hydrotreating catalysts. *J. Catal.* **2006**, *237*, 118–130. [CrossRef]
24. Perevoznikov, S.S.; Tsybulskaya, L.S. Effect of structure of electrodeposited nickel-phosphorous coatings on their physico-mechanical and corrosion-protective properties. *Electroplat. Surf. Treat.* **2020**, *28*, 10–20. [CrossRef]
25. Ganavati, A.; Kukareko, V.A.; Tsybul'skaya, L.S. Strukturnoe sostoyanie i iznosostoikost' pokrytii Ni-P. *Sovrem. Metod. Tekhnologii Sozdaniya Obrab. Materialov. Sb. Nauchnikh Tr.* **2014**, *B*, 68–79.
26. Xing, F.; Zhao, B.; Shi, W. Study on tunable fabrication of the ultra-black Ni–P film and its blacking mechanism. *Electrochim. Acta* **2013**, *100*, 157–163. [CrossRef]
27. Liu, Y.; Beckett, D.; Hawthorne, D. Effect of heat treatment, top coatings and conversion coatings on the corrosion properties of black electroless Ni–P films. *Appl. Surf. Sci.* **2010**, *257*, 4486–4494. [CrossRef]
28. Perevoznikov, S.; Ivanovskaya, M.I.; Tsybul'Skaya, L.S.; Gaevskaya, T.V. Infrared spectroscopy of ultrablack films based on electrodeposited Ni–P alloys. *J. Appl. Spectrosc.* **2014**, *81*, 592–596. [CrossRef]
29. Johnson, C.E. Ultrablack Coating Due to Surface Morphology. U.S. Patent PB-81-131526, 4 June 1980.
30. Stinner, C.; Tang, Z.; Haouas, M.; Weber, T.; Prins, R. Preparation and 31P NMR characterization of nickel phosphides on silica. *J. Catal.* **2002**, *208*, 456–466. [CrossRef]
31. Bekaert, E.; Bernardi, J.; Boyanov, S.; Monconduit, L.; Doublet, M.-L.; Ménétrier, M. Direct correlation between the 31P MAS NMR response and the electronic structure of some transition metal phosphides. *J. Phys. Chem. C* **2008**, *112*, 20481–20490. [CrossRef]
32. Atkinson, R.J. Nuclear Magnetic Resonance in Some Pyrophosphates. Ph.D. Thesis, McMaster University, Hamilton, ON, Canada, 1969.
33. Berhault, G.; Afanasiev, P.; Loboué, H.; Geantet, C.; Cseri, T.; Pichon, C.; Guillot-Deudon, C.; Lafond, A. In Situ XRD, XAS, and magnetic susceptibility study of the reduction of ammonium nickel phosphate $NiNH_4PO_4 \cdot H_2O$ into nickel phosphide. *Inorg. Chem.* **2009**, *48*, 2985–2992. [CrossRef] [PubMed]